The paper was published in the proceedings of the 11th International Conference on Physical Modelling in Geotechnics (ICPMG2026) and was edited by Ioannis Anastasopoulos. The conference was held from June 8th to June 12th 2026 in Zurich, Switzerland.

Proceedings of the 11th ICPMG 2026
11th International Conference on Physical Modelling in Geotechnics
8-12 June 2026, Zurich, Switzerland

Preliminary insights into an innovative vibratory–jetting pile installation method

C. Cengiz
Deltares, Delft, the Netherlands, cihan.cengiz@deltares.nl

M. Konstantinou, A. Rodríguez Piedrabuena, G. Macaro
Deltares, Delft, the Netherlands, maria.konstantinou@deltares.nl, alba.rodriguezpiedrabuena@deltares.nl, giulia.macaro@deltares.nl

C.J.W. van Verseveld, H. Köpüklü
GBM Works, Amsterdam, the Netherlands, c.vanverseveld@gbmworks.com, h.kopuklu@gbmworks.com

ABSTRACT: The Silent Installation of MonoPiLEs III (SIMPLE III) project investigated the influence of vibratory and Vibrojet® installation methods on soil behaviour around monopile analogues in a controlled 2D soil container. While the companion contribution focuses on the development of the pile installation setup, this paper presents the first results of an extensive instrumentation program, designed to quantify soil state changes around the pile during pile penetration. The measurement system included pore pressure transducers, total stress cells, a camera, and conductivity-type concentration meter (CCM) sensors, the latter providing non-destructive monitoring of porosity evolution in saturated granular media. Calibration of the CCM probes allowed porosity changes to be tracked continuously with depth and time. Results demonstrate that pile penetration induces distinct phases of soil response when the jetting flow remains within the pile: (i) an initial local loosening as the pile approaches the measurement zone, followed by (ii) progressive densification once the tip advances within a certain distance to the measuring point. These trends were consistently captured in both fine and medium sands at various densities across vibratory and Vibrojet® conditions. Integrated analysis of CCM, pile penetration and hook load data confirms that while an initial loosening occurs along the shaft, the net effect of installation is a densification of the surrounding soil. The study also exhibits the value of CCM sensors as a robust tool for real-time monitoring of porosity changes during installation processes which enable improved interpretation of soil-structure interaction mechanisms relevant for offshore monopile foundations.

1 INTRODUCTION

The offshore wind industry is becoming increasingly aware of its methods and their impacts on the ecosystem. Currently, almost all regulating bodies have measures in place to mitigate or limit the impact of offshore developments on the marine life. Beyond the regulations, there are a multitude of engineering solutions to lessen the impact of renewable energy construction on the environment (Koschinski and Lüdemann 2020). Preferably, disturbance is limited not only by mitigation measures but by adopting methods that inherently minimise environmental impact. The vibratory–jetting technique investigated here (Vibrojet®) uses a controlled internal jet to assist pile penetration, which reduces seabed disturbance and lowers the overall footprint of piling operations.

From a purely physics point of view, it is readily established that fluidisation of a granular assembly reduces the force required to penetrate an intruder to a granular assembly (Liu et al. 2019). This principle is also applied within the realm of geotechnical engineering and several studies have investigated the benefits of utilising a water jet to install pile-like elements into soil beds. According to early reports, the use of water jets for pile installation was a long established construction practice, as seen in the accounts by Tsinker in the 1970s (Tsinker 1977; Tsinker 1988). Although the literature trail is incomplete, some researchers cite earlier work from the former USSR in the 1960s (Shestopal 1959). Following these early studies, modern-day engineering practice has also investigated the feasibility of using water jets in offshore construction. de Brum Passini et al. (2016) ran a series of laboratory tests to study the embedment depth of so-called torpedo piles. In follow-on studies, de Brum Passini et al. (2018) investigated the jet-induced fluidisation mechanism in saturated sand and its control on embedment depth for torpedo piles.

Dong (2022) further expanded the use of jetting for torpedo piles by including mechanical vibrations to assess the penetration aspects into cohesive sedimentary beds.

The fluidisation concept was also explored for piles. Gabr et al. (2013) used partial jetting to aid the installation of piles through relatively shallow hard subsurface soil layers. This was primarily done to minimise their exposure to excessive driving stress and provide energy savings and noise reduction. Schnaid et al. (2014) carried out laboratory measurements and found that fluidisation geometry is controlled by combined effects of jet velocity and the ratio of particle and jet diameters. They have also observed a considerable reduction of relative density of fluidised zones. Maiti and Shepley (2025) performed a series of pile installation tests and proposed a force-balance model to quantify the penetration depth of the pile under a critical jetting velocity.

Despite these efforts, the precise control of the jetting to minimize the state change in the peripheral soil was not investigated in prior studies. General trend in the presently available literature is a vastly softened peripheral soil body around the pile as reported by (Alsaydalani and Clayton 2014). A fluidised region develops around the jet, forming an annular ring of mobilised particles around the pile. Inside this zone, grains exhibit increased mobility and partial suspension due to jet pressure and convective flow generated by the high-velocity jet. Outside the fluidised region, the jet decelerates to velocities too low to move grains, and the fluid simply permeates deeper into the bed (Maiti and Shepley 2025). In itself, loosening of the soil around the intruder is harmless and even expected. However, as the pile utilises the strength and stiffness from the soil in its immediate vicinity to derive lateral restraint, it becomes imperative to mitigate adverse effects of jetting in this zone. This is especially true for monopiles as most of the load demand is in the lateral direction throughout the design-life of the structure.

The present contribution outlines the laboratory testing program which elaborates on an exemplar sub-set of the tests conducted within the SIMPLE III experimental (laboratory scale) program. The exemplar tests are selected to demonstrate the effects of vibro-jetting on the soil state of the peripheral soil outside of the piles.

2 LABORATORY TESTS

The details of the experimental program, the test setup, and instrumentation are elaborated in the companion paper which is also presented in the ICPMG 2026 and published in the conference proceedings (van Verseveld et al. 2026). Table 1 shows the sub-set of selected experiments and their properties. While the first four tests are selected to demonstrate the effects of vibro-jetting with different flow control parameters, the last three tests are added to demonstrate the vibro-jetting effects on different soil beds when the jetting flow is maintained within the pile.

Table 1. A tabulated list of the experiments and their properties.

Test Number	Sand type	D_r (%)	Flow in Pile*
324-01	Fine	80	No Flow
324-02	Fine	80	Within
335-01	Fine	80	Within (higher flow)
335-02	Fine	80	Underflow
343-02	Fine	60	Within
311-02	Medium	80	Within
321-03	Medium	60	Within

* No Flow: The pile analogue is only penetrated with vibrations; Within: The jetting is controlled such that the jet does not exceed the pile tip; Underflow: Deliberate over-jetting to create underflow conditions.

2.1 Testing Assembly and Instrumentation

Figure 1 illustrates the testing assembly and its main features. The setup is heavily instrumented with a wide range of sensors and assembly components as marked on Figure 1. The left-most entity in Figure 1 is the pile-hammer assembly and at the top elevation, a loadcell is used as connection interface to the crane so that the so-called hook-loads can be measured. The orange blocks represent the vibro-hammer used in the study and the 268.8 cm long portion is the planar pile analogue that is used to penetrate into the granular soils. The pile-analogue is rotated 90 degrees such that thin side is visible through the glass wall of the experimental assembly (the blue line resembles where the pile would go through during the tests).

2.2 Measurement of Porosity – CCM Sensors

A dedicated section is reserved here to explain the Concentration Conductivity Measurement (CCM) sensors and for further details, interested readers are referred to Cengiz et al. (2025). CCM sensors are used to quantify porosity by recording bulk electrical conductivity and mapping it to formation factor using Archie-type relationships. Silica sands are effectively non-conductive; hence, as grain volume fraction increases, bulk conductivity decreases. The conductivity of the sand–water mixture scales with the pore-water conductivity which enables porosity inference from their ratio. CCM measurements are non-destructive, deployable in arrays, and suitable for high-frequency logging, while relying on simple electronics compared with wave-based methods. In the present 2D container, which is only 300 mm wide, alternative in-situ techniques were impractical for resolving local state changes; therefore, the Deltares-developed CCM method was adopted to track porosity and density evolution during installation.

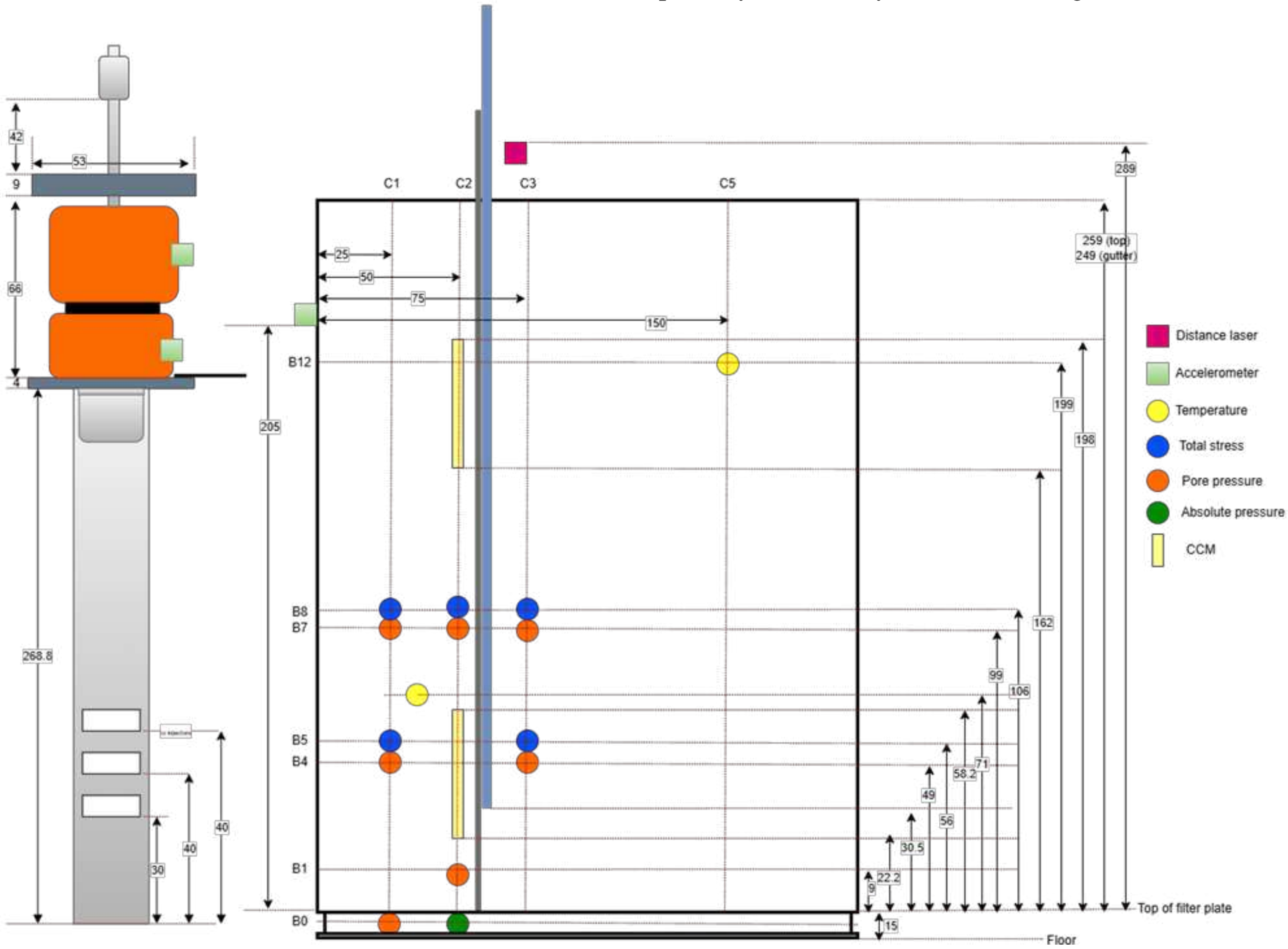

Figure 1. Instrumentation layout used in the tests, all dimensions are in cm; blue line represents the pile at target depth. For more information, please refer to the companion paper presented in the proceedings of ICPMG 2026 (van Verseveld et al. 2026)

2.3 Geo-Materials

The experimental program utilised two different commercially available sands. These are S90 and M31 sands, which are supplied by Sibelco GmbH. The grain size distributions of these materials are illustrated in Figure 2. The index properties of these materials, alongside with the USCS classification, are tabulated in Table 2. Both S90 and M31 sands are classified as 'poorly graded' (SP) sands. Furthermore, Figure 3 illustrates the microscope images of the used sands.

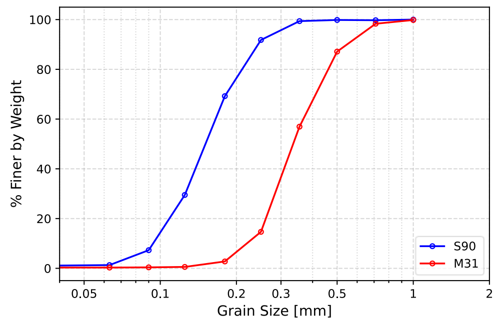

Figure 2. Grain size distribution curves for S90 and M31 sands.

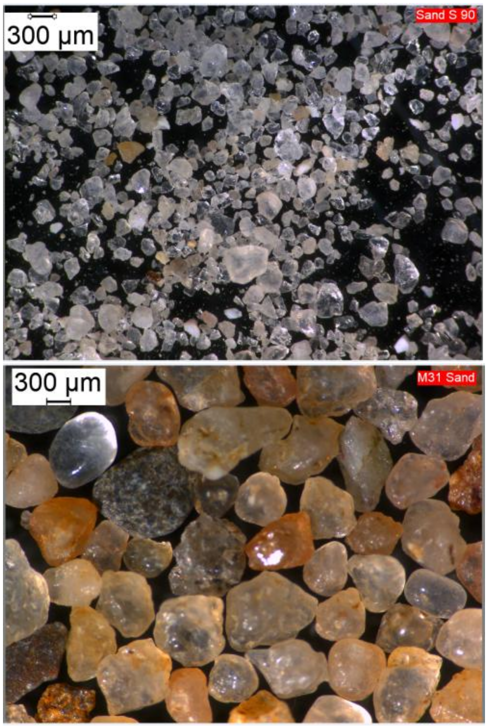

Figure 3. Microscope images of the sands used.

Table 2. Properties of the sand materials used.

Properties	Sands	
	S90	M31
G_s	2.66	2.65
e_{min}	0.64	0.49
e_{max}	0.93	0.76
D_{10} (mm)	0.09	0.22
D_{30} (mm)	0.12	0.28
D_{60} (mm)	0.16	0.36
c_u	1.78	1.64
c_c	1.01	0.99
USCS	SP	SP

3 RESULTS

3.1 Pile Installation Data

Figure 4 illustrates the installation time-history of the pile in terms of vertical (installation) displacement and hook load for an exemplar test, which is the second entry in Table 1, Test 324-02. The installation process for each test began while the pile-hammer assembly was free-hanging, therefore the initially recorded value is the dead-weight of the entire assembly. The vibratory hammer is engaged during the free-hanging period before the pile-hammer assembly was lowered to initiate penetration. In each test, a target penetration depth of 850 mm into the sand is adopted.

Out of the two CCM sensor array locations, the lower one, named CCM-2, is used in the herein presented comparison of the porosity changes due to pile installation. The CCM-2 location is illustrated in Figure 5 and it starts at 582 mm above the base of the setup as per the sketch in Figure 1 and the CCM array houses 10 discrete measurement locations separated by 40 mm, numbered CCM 2-1 to CCM 2-10 from top to bottom. The image shown in Figure 5 is taken during the dismantling of the setup.

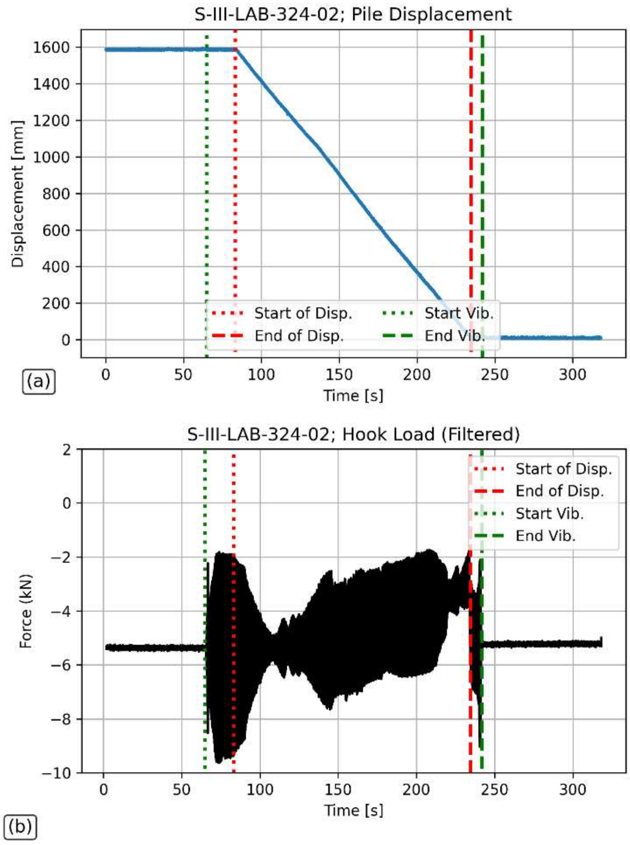

Figure 4. (a) Pile penetration time history and (b) hook-load time history for an exemplar test. The vertical displacement represents the distance of the pile tip to target depth, the latter which is approximately 850 mm into the sand sample.

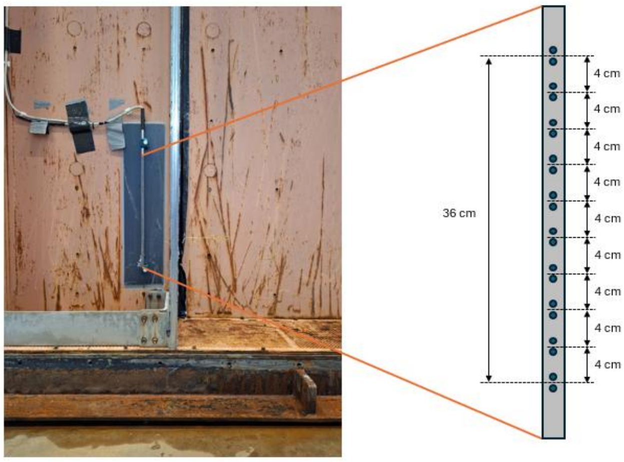

Figure 5. A photograph of the and a sketch of the CCM-2 sensor array containing 10 discrete measurement points with two pairs of circular electrodes.

Using the exemplar test elaborated above (Test 324-02), the soil porosity change in time domain is illustrated in Figure 6. An initial loosening of the soil is observed upon initiation of the vibro-hammer as seen by the minute spike following the green dotted line. At the end of penetration, represented by the red dashed-line, the porosity values reach to a local minimum. The vibratory movement is subsequently seized by turning off the vibro-hammer.

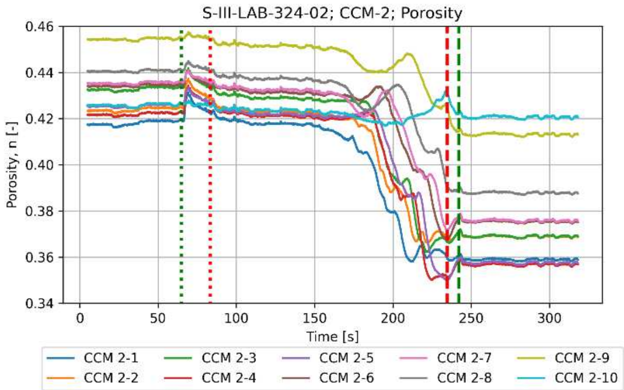

Figure 6. Time-domain CCM readings for test 324-02.

Figure 7 further illustrates the stress state changes in the soil due to pile installation with jetting. The overall response of the soil is densification with significant decreases in porosity. It is seen that as the pile tip approaches the measurement location, the porosity shows an initial decrease followed by (in some cases) an increasing trend . Following this, as the pile tip comes closer to the monitored area, the porosity decrease (density increase) significantly increases, which starts at approximately the same distance from the pile tip for all the individual measurement locations.

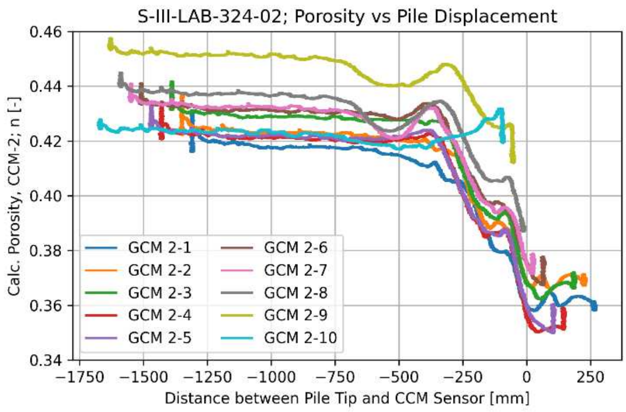

Figure 7. Plots of porosity as a function of the pile tip distance from the measurement point.

Figure 8 illustrates the net porosity change measured by the CCM-2 sensor for all tests summarised in Table 1. The bar plot illustrates the average porosity at the beginning and end of the pile penetration which corresponds to the red vertical lines in the previous plots (t_1 beginning of displacement and t_2 end of displacement). The error bars represent the band of the variance in the measured quantities with the CCM sensor's individual measurement locations. A deeper look into the densification phenomena is provided in Figure 9 where a scatter plot of the initial porosity at t_1 is plotted against the final porosity at t_2. From these plots it is evident that the vibro-jetting method has a net porosity decrease (or density increase) effect on the considered sands. This observation is true with the notable exception of the Test 355-02, where the flow was deliberately increased to cause underflow conditions. For all tests conducted within the experimental program reported herein or otherwise, the flow conditions were controlled precisely to yield desired flow regimes within the pile. The underflow condition is induced by voluntary control to test the outcomes of underflow state.

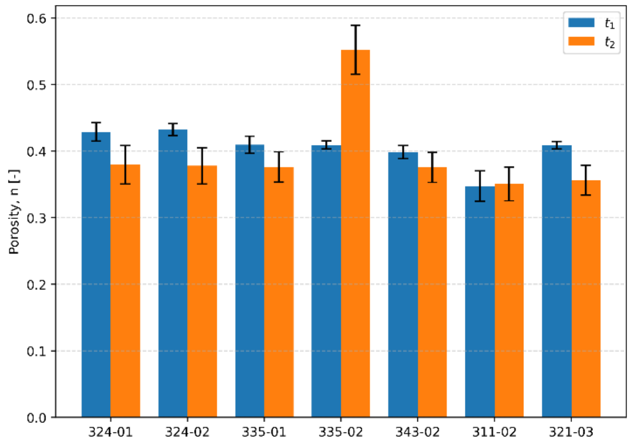

Figure 8. Bar plot of the average porosity of sands as measured by CCM-2 sensor.

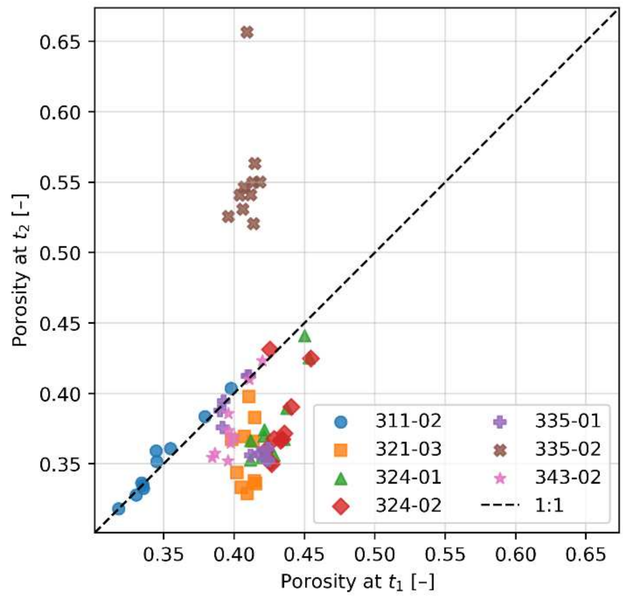

Figure 9. Scatter plot of the initial versus final porosities.

4 CONCLUSIONS

Across all tests, pile penetration exhibited a two-phase response: a brief local loosening as the tip approached the sensor plane, followed by clear densification once the tip came close to the measurement location or passed by it. The net outcome was a reduction in porosity around the shaft in both fine and medium sands and at different densities; persistent loosening was observed only under deliberate underflow jetting. Keeping the jet within the pile tip limited peripheral fluidisation compared with excerssive (underflow) jetting. In the 300 mm wide 2D container, CCM arrays were essential to capture state changes non-destructively and at high rate. Practically, controlled vibratory–jetting is expected to deliver a stiffer initial lateral response for monopiles by preserving near-shaft densification. The study is constrained by plane-strain, thin-tank conditions and specific materials; future work should quantify wall and drainage effects, expand the jet-control parameter space, and translate porosity changes into design modifiers (e.g., p–y initialisation).

ACKNOWLEDGEMENTS

The experimental set-up was designed by GBM Works in cooperation with Deltares and operated at the Deltares laboratory as part of the SIMPLE IIB and SIMPLE III GROW Joint Industry Projects. Funding from Topsector Energiesubsidie van het Ministerie van Econsomische Zaken under RVO grant number HER+21-02575541 and HER+22-02-03441592 and the following partners (alph.) are gratefully acknowledged: Atlantic Shores Offshore Wind, CAPE Holland, Carbon Trust (BP, Parkwind, TotalEnergies), DEME Offshore, Ecowende, EnBW, Eneco, RWE, Seaway7, Shell, TNO, Van Oord, Vattenfall and Waterkant Energy.

REFERENCES

Alsaydalani, M., and Clayton, C. (2014). "Internal fluidization in granular soils." Journal of Geotechnical and Geoenvironmental Engineering, 140(3), 04013024. https://doi.org/10.1061/(ASCE)GT.1943-5606.0001039

Cengiz, C., Konstantinou, M., Harkes, M., Boonstra, D., Piedrabuena, A. R., and Talmon, A. (2025). "Application of concentration conductivity measurement (CCM) for porosity and density profiling in granular media." Measurement, 116644. https://doi.org/10.1016/j.measurement.2025.116644

de Brum Passini, L., Schnaid, F., and Rocha, M. M. (2016). "MECHANISMS AND GEOMETRY OF PILE INSTALLATION BY WATER JET FLUIDIZATION IN FINE SAND."

de Brum Passini, L., Schnaid, F., Rocha, M. M., and Möller, S. V. (2018). "Mechanism of model pile installation by water jet fluidization in sand." Ocean Engineering, 170, 160-170. https://doi.org/10.1016/j.oceaneng.2018.10.017

Dong, C. (2022). "Torpedo pile penetration by combined water jet and mechanical vibrations in cohesive sedimentary beds." Ocean Engineering, 266, 112723. https://doi.org/10.1016/j.oceaneng.2022.112723

Gabr, M., Borden, R., Denton, R., and Smith, A. (2013). "An insertion rate model for pile installation in sand by jetting." Geotechnical Testing Journal, 37(1), 13-23. https://doi.org/10.1520/GTJ20120191

Koschinski, S., and Lüdemann, K. (2020). "Noise mitigation for the construction of increasingly large offshore wind turbines." Technical Options for Complying with Noise Limits, 40.

Liu, C.-P., Bai, S., and Wang, L. (2019). "Resistance forces on an intruder penetrating partially fluidized granular media." Physical Review E, 99(1), 012903.

Maiti, R., and Shepley, P. (2025). "Penetration of jet piles on submerged granular beds." Ocean Engineering, 315, 119914.

Schnaid, F., Passini, L., Stracke, F., and Mezzomo, S. (2014). "On the response of fluidized piles from laboratory model tests in granular soils." Journal of Geo-Engineering Sciences, 1(2), 69-81. https://doi.org/10.3233/JGS-140024

Shestopal, A. (1959). "Jetting of pipes, piles, and sheet piles." Hydro project institute.

Tsinker, G. P. (1977). "Performance of jetted anchor piles with widening." Journal of the Geotechnical Engineering Division, 103(3), 213-226.

Tsinker, G. P. (1988). "Pile jetting." Journal of geotechnical engineering, 114(3), 326-334. https://doi.org/10.1061/(ASCE)0733-9410(1988)114:3(326)

van Verseveld, C. J. W., Dasselaar, S. J., Griffin, L., Apetroae, A. M., Cengiz, C., Rodriguez Piedrabuena, A., Konstantinou, M., and Macaro, G. "Plane-strain apparatus to study the effect of Vibrojet® pile installation on soil state." Proc., 11th International Conference on Physical Modelling in Geotechnics (ICPMG).